Mesospheric signatures observed during 2010 minor stratospheric warming at King Sejong Station (62°S, 59°W)

S. Eswaraiah [a,b], Yong Ha Kim [a,*], Junseok Hong [a], Jeong-Han Kim [c], M. Venkat Ratnam [d], A. Chandran [e], S.V.B. Rao [f], Dennis Riggin [g]

[a] Department of Astronomy, Space Science and Geology, Chungnam National University, Daejeon, South Korea
[b] Sri Venkateswara College of Engineering, Vidyanagar, Bangalore, India
[c] Korea Polar Research Institute, Incheon, South Korea
[d] National Atmospheric Research Laboratory (NARL), Gadanki, Tirupati, India
[e] Laboratory for Atmospheric and Space Physics, University of Colorado, Boulder, CO, USA
[f] Department of Physics, Sri Venkateswara University, Tirupati, India
[g] Global Atmospheric Technologies and Science, Inc. (GATS), Boulder, CO 80301, USA

ARTICLE INFO

ABSTRACT

A minor stratospheric sudden warming (SSW) event was noticed in the southern hemisphere (SH) during September (day 259) 2010 along with two episodic warmings in early August (day 212) and late October (day 300) 2010. Among the three warming events, the signature of mesosphere response was detected only for the September event in the mesospheric wind dataset from both meteor radar and MF radar located at King Sejong Station (62°S, 59°W) and Rothera (68°S, 68°W), Antarctica, respectively. The zonal winds in the mesosphere reversed approximately a week before the September SSW event, as has been observed in the 2002 major SSW. Signatures of mesospheric cooling (MC) in association with stratospheric warmings are found in temperatures measured by the Microwave Limb Sounder (MLS). Simulations of specified dynamics version of Whole Atmosphere Community Climate Model (SD-WACCM) are able to reproduce these observed features. The mesospheric wind field was found to differ significantly from that of normal years probably due to enhanced planetary wave (PW) activity before the SSW. From the wavelet analysis of wind data of both stations, we find that strong 14–16 day PWs prevailed prior to the SSW and disappeared suddenly after the SSW in the mesosphere. Our study provides evidence that minor SSWs in SH can result in significant effects on the mesospheric dynamics as in the northern hemisphere.

1. Introduction

Numerous studies have been done on stratospheric sudden warmings (SSW) and their possible dynamical impacts on the mesosphere, especially in the northern hemisphere (NH) (Charlton and Polvani (2007), Kishore et al. (2012), De la Torre et al. (2012) and references there in). However, such studies are relatively few in the southern hemisphere (SH) (Baldwin et al., 2003; Hoppel et al., 2003; Shepherd et al., 2005; Dowdy et al., 2004; Mbatha et al., 2010). SSWs are less frequent in the SH and this hemispheric disparity may be attributed to less topographic forcing of planetary waves (PWs) (Andrews et al. (1987), Chandran et al. (2014) and references there in). According to the World Meteorological Organization (WMO) definition, minor SSWs are events having

reversal of temperature gradient at 10 hPa pole ward of 60°, while major warmings, in addition to the temperature gradient reversal, require reversal of the mean zonal wind to westward at 60° (Labitzke and Naujokat, 2000; Chandran et al., 2014). Minor SSWs are seen more frequently than major SSWs in the SH and one such minor SSW was observed in 2010 (Chandran et al., 2014). Earlier studies (Coy et al., 2005; Siskind et al., 2010; Chandran et al., 2013) on minor warmings have stressed their effects on the mesosphere. The disturbed winter conditions cause profound effects on stratospheric ozone densities that are greatly reduced especially during major warmings in the NH (Manney et al., 2009). A similar effect was also observed in the SH during the recent 2010 minor warming (de Laat and van Weele, 2011).

The first observational study on SSWs was made over 60 years ago (Scherhag, 1952). However, there are still advances to be made in the understanding of SSW effects on atmospheric dynamics, coupling and composition. It is generally accepted that SSWs are produced by the interaction of PW with mean flow in the

* Corresponding author.
 E-mail address: yhkim@cnu.ac.kr (Y.H. Kim).

stratosphere (Matsuno, 1971). This interaction decelerates and even reverses the zonal mean eastward winter stratospheric jet and forces poleward/downward flow in the winter-time polar stratosphere resulting in adiabatic heating in the stratosphere. At the same time, the slow/reversed stratospheric jet reduces/reverses the normal westward gravity wave forcing in the winter polar mesosphere. The net eastward forcing due to gravity wave breaking in the MLT, resulting in zonal wind reversal from westward to eastward. The associated mean residual circulation changes from downward to upward, leading to gravity wave induced adiabatic cooling in the mesosphere (Liu and Roble, 2002; Chandran et al., 2014).

At high-latitudes, in general, the stratospheric and mesospheric winds and temperature can be subjected to significant changes during disturbed winters (Liu and Roble, 2002; Cho et al., 2004). Mesospheric cooling (MC) has been reported for both hemisphere during major SSW events; in the NH, Cho et al. (2004) documented the MC using the ground-based Spectral Airglow Temperature Imager and in the SH using the OH and O_2 airglow observations by Azeem et al. (2005). MC has also been detected during minor SSW (sometimes also referred to as Upper Stratosphere Lower Mesosphere (USLM) disturbances) in lidar, Michelson interferometer, rocketsondes, satellite radiometry and meteorological analyses (Labitzke, 1972; Fairlie et al., 1990; Greer et al., 2013; Thayer and Livingston, 2008; Siskind et al., 2005; von Zahn et al., 1998). Recently de Wit et al. (2015) noticed cooling about 10 km below the mesopause over Trondheim, Norway (63°N, 10°E) using the MLS temperature data for the January 2013 major SSW.

Using long-term (1979–2006) satellite observations, Hu and Fu (2009) demonstrated that the occurrence rate of SSW in SH is maximized in the late winter and spring season (September–October) by temperature increase up to ~ 7 to 8 °C. They also showed a close correlation between SSW in SH and increase of sea surface temperature (SST) as a consequence of the increasing greenhouse gasses due to anthropogenic activity.

In the SH, the only reported major SSW event occurred in 2002 (Baldwin et al., 2003) and its impact on mesospheric dynamics was well studied by Dowdy et al. (2004) using simultaneous MF radars over Antarctica region and by, Mbatha et al. (2010) with HF radar. In the context of planetary waves and tide interaction, mesospheric winds have been studied with a meteor radar at Rothera (68°S, 68°W) by Mthembu et al. (2013). However, the impact of minor SSW events on mesospheric dynamics has only been studied to a limited degree in both hemispheres, except a few model simulations (Siskind et al., 2010; Chandran et al., 2013). To the best of our knowledge no experimental study, especially with meteor radar data, has been reported for the influence of minor SSW on the SH mesospheric dynamics.

Here, we present the mesosphere features over the Antarctica region during a minor SSW event, which occurred in September 2010. We analyze the mesospheric winds and occurrence of MC in conjunction with the minor SSW by using simultaneous measurements of a meteor radar at King Sejong Station (KSS) (62°S, 59°W) and a Rothera MF radar, together with the Microwave Limb Sounder (MLS) temperature measurements. Furthermore, we verify the dynamical response of the polar mesospheric region for the 2010 minor SSW with a simulation of a global circulation model (GCM), which shows a clear link between stratosphere and mesospheric region. Section 2 provides the data used in the present study, the results and discussion are given in Section 3, followed by the summary in Section 4.

2. Data

2.1. Mesospheric radar data

In the present study, we use combined observations of King Sejong Station Meteor Radar (hereafter called KSS MR) and Rothera MF radar (MF radar), which provide wind information in the mesospheric region during the period of 2007–2014.

The meteor radar was installed in March 2007 near the tip of Antarctica peninsula (Kim et al., 2010), and has been operated in all-sky interferometric mode with 1 transmitting antenna and 5 receiving antennas at 33.2 MHz. The radar transmitted with a maximum peak power of 8 kW until March 2012 and the power was upgraded to 12 kW afterward. The wind measurement technique is similar to the standard method given in Holdsworth et al. (2004) and the radar provides winds at altitudes of 80–98 km at 1 h and 2 km resolutions (Lee et al., 2013).

Rothera MF Radar is a coherent, spaced-antenna system and has been operated since 1997 (Jarvis et al., 1999). The radar employs a single broad-beam transmitting antenna and three spaced receiving antennas in a triangular array. The radar operates with a transmitting power of 25 kW at a frequency of 1.98 MHz (Hibbins et al., 2007) and provides winds in the mesosphere and lower thermosphere at 4 km altitude resolution every hour and these data were re-sampled to 2 km height resolution. The winds measured by a MF radar are usually in agreement with those measured by a meteor radar up to an altitude of ~ 94 km, above which a MF radar tends to underestimate the winds compared to those observed by a meteor radar (Manson et al., 2004; Portnyagin et al., 2004; Rao et al., 2014). In the present study we made use of winds at 82 km to characterize the mesosphere response to the 2010 minor SSW.

2.2. EOS MLS data

The Earth Observing System (EOS) Microwave Limb Sounder (hereafter called MLS) is one of the four instruments aboard NASA's Aura satellite, launched on 15 July 2004. The MLS is a radiometer that retrieves temperature from bands near the O_2 spectral line at 118 and 239 GHz. It measures temperatures at 316–0.001 hPa pressure levels with a track resolution of 230 km for global coverage from 82°S to 82°N with ~ 15 orbits per day, providing ~ 30 samples daily for given latitude. The vertical resolution is 3 km at 31.6 hPa, degrading to 6 km at 316 hPa and to ~ 13 km at 0.001 hPa. Details of the MLS and temperature validation are given in Schwartz et al. (2008). In the present study, we have used the zonal mean temperatures derived at 80°S.

2.3. ERA-interim database

We also make use of stratospheric zonal mean zonal winds and temperatures obtained from ERA-Interim reanalysis (Dee et al., 2011) datasets provided by the European Center for Medium-range Weather Forecasts (ECMWF). ERA-Interim is the latest global atmospheric reanalysis dataset produced by the ECMWF for the period from 1 January 1979 onwards (http://www.ecmwf.int/en/research/climate-reanalysis/era-interim). The ERA-Interim dataset covering the pressure levels 1000 and 1 hPa (~ 0–48 km) with a latitudinal and longitudinal grid of 1.5° × 1.5° is used in this study, though higher spatial resolutions are now available. The data set consists of results from reanalysis conducted at six-hour intervals at 1.5° latitude–longitude resolution, using both ground-based and space-born observations. In the present study we have utilized zonal mean temperature and zonal winds at 10 hPa.

2.4. The whole atmosphere community climate model (WACCM)

The WACCM is a general circulation model (GCM), developed at the National Center for Atmospheric Research (NCAR). The model is derived from the Community Atmosphere Model (CAM3) and is a fully coupled chemistry–climate model (Garcia et al. (2007) and references therein). The model domain extends from the Earth's surface to ~ 145 km (4.5×10^{-6} hPa) and has a horizontal resolution of $1.9° \times 2.5°$ (latitude × longitude). Usually the warming events generated in GCMs in the SH rarely fulfill the WMO criteria for either major or minor events due to the existence of strong SH jets in winter, commonly referred to as the cold pole problem in climate models (Marsh et al., 2013), which is a limitation of current GCMs. The WACCM has been extensively used for studying SSW events that occurred in the NH, such as the 2006 and 2009 major SSW (Chandran et al., 2014) and the 2012 minor SSW (Chandran et al., 2013). For these studies a "specified dynamics" version of WACCM (termed as SD-WACCM) is run with the model dynamical and temperature fields in the troposphere and stratosphere constrained by relaxing the horizontal winds and temperatures to GEOS-5.2 reanalysis data from the surface to 40 km (Rienecker et al., 2008). SD-WACCM resolves large-scale waves, including planetary waves, but the effect of mesoscale orographic and non-orographic small-scale gravity waves is parameterized in the model (Garcia et al., 2007; Richter et al., 2010). In the present study, a SD-WACCM simulation has been used to evaluate the 2010 SSW in SH and to study the coupling between the stratosphere and mesosphere.

3. Results and discussion

3.1. Characteristics of 2010 minor SSW in SH

Fig. 1 shows daily zonal mean zonal wind at 60°S and temperature difference between 60°S and 90°S obtained from ERA-Interim reanalysis dataset for the year 2010 at 10 hPa. It is clear from the figure that during 2010 SH winter, a clear minor warming event occurred in mid September (day 259) marked with a dashed vertical line. In addition to the September minor warming two other episodic warmings were also noticed in early August (day 212) and late October (day 300). According to WMO criteria for minor SSW, reversal of temperature gradient at 10 hPa poleward of 60° should exist (Labitzke and Naujokat, 2000). During the September (day 259) event, the temperature gradient reverses and is near zero (Fig. 1). The August warming does not show sharp increase in temperature, and the October warming should be considered as episodic increase overlapped with a seasonal trend

indicative of a final warming. The zonal wind was weakened by ~ 20 to 25 m/s during the September warming, but the winds at the other warmings were not weakened as much. In addition, these two warmings are not associated with planetary wave activities, which will be discussed later.

For verification of the 2010 SH minor SSWs, an SD-WACCM simulation has been performed and is presented in Fig. 2. The SD-WACCM simulation clearly captures the warming events that were observed in ERA-Interim reanalysis (Fig. 1). The simulated zonal mean zonal winds at 60°S are plotted in Fig. 2a, which shows clear weakening of zonal winds during the September event. Fig. 2b depicts zonal mean temperatures averaged over the polar cap between 75°S and 90°S. The simulation shows that during the September event the warm stratopause descended to 40–45 km coinciding with cooling in the mesosphere. However, during the August event the warm stratopause descended but not below 45 km, and the stratopause change very little during the October event. Usually during an undisturbed winter the NH stratopause altitude lies at 55–60 km, whereas it descends to 38–41 km during SSWs (Chandran et al., 2014). In contrast, in SH the stratopause remains at 65–70 km during quiet winter, and descends to 45–50 km during SSW (Pan and Gardner, 2003; Kawahara et al.,2004). By considering the cold pole problem in climate model simulations, Chandran et al. (2014) used a new criterion for detecting minor warmings in the SH: the positive temperature gradient between 60°S and 90°S exists at 45–50 km, and the zonal mean zonal wind weakens by $\sim 50\%$ but does not reverse at 45 km. The September event satisfies these conditions.

3.2. Mesospheric mean wind structure during 2010

Figs. 3 and 4 exhibits the daily average hourly zonal and meridional winds, respectively, from the start of July until the end of December 2010 observed at KSS MR and Rothera MF radar. The background wind contains both gravity waves and tides. It is clear from the figures that both zonal and meridional winds at these two locations show strong similarities, except that the Rothera winds are weaker than those from KSS MR at higher altitudes as expected (Rao et al., 2014). Since, the two radars are separated only by 8° latitude, significant difference in winds is not expected (Dowdy et al., 2004), which is confirmed in these figures. The mesospheric semiannual oscillation (MSAO) is evident in zonal winds up to an altitude of 85 km in KSS meteor radar observations and 90 km in MF radar, as winds are dominantly eastward in winter (up to October) and then become westward (November and December) in summer. The difference in MSAO between the two radar observations is due to the wind measuring technique and altitude coverage of radar observations. Above 85 km the magnitude of eastward
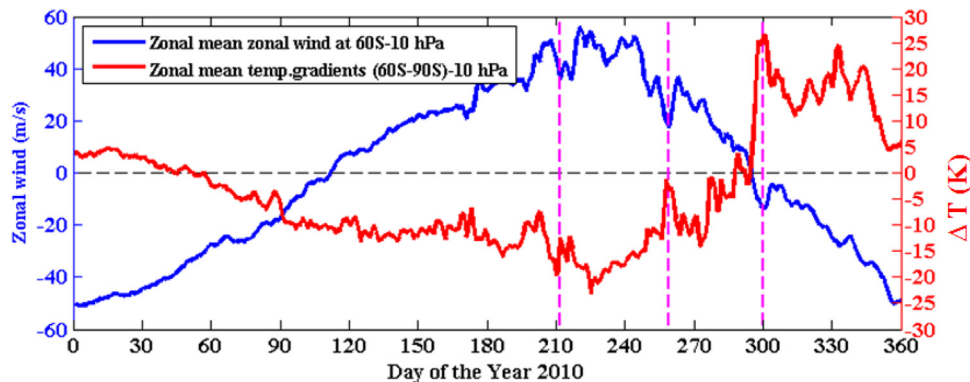

Fig. 1. Daily zonal mean zonal wind (blue line) at 60°S and temperature difference (60°S and 90°S) (red line) obtained at 10 hPa from ERA-Interim re-analysis dataset for the year 2010. Axis for the temperature is given at the right. The vertical dashed line indicates the day of peak warming and the dashed horizontal line is for the zero wind level. (For interpretation of the references to color in this figure legend, the reader is referred to the web version of this article.)
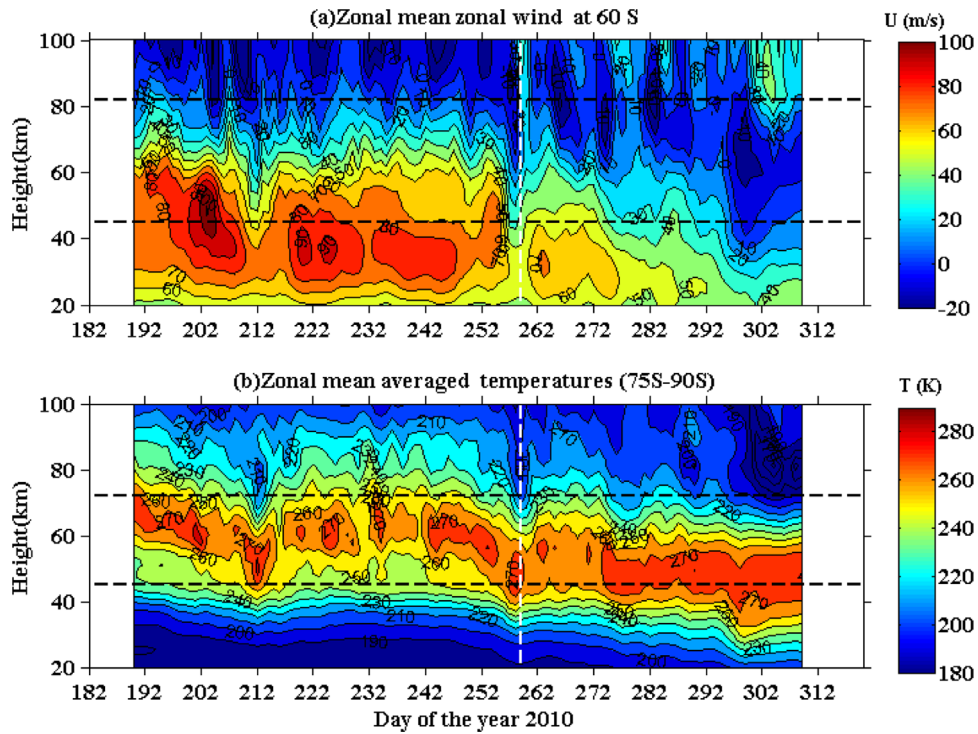
Fig. 2. Zonal mean (a) zonal winds at 60°S and (b) average temperature (75–90°S) from day 190 to 310 in 2010 from the SD-WACCM simulation. Vertical dashed line indicates the day of peak warming. Dashed horizontal lines in (a) indicate the 1 hPa (45 km) level and 82 km, and those in (b) are for the altitudes of 45 km and 72 km.

wind is lower in both the radar observations during winter. SD-WACCM simulations reflect this effect more drastically showing westward winds above 85 km (Fig. 2a). It should be noted that single site observations of mesospheric winds often show discrepancy with GCM output. The wind reversal in the mesosphere is a gravity wave driven phenomena and gravity wave

parameterizations employed in GCMs often do not capture local gravity wave induced mesospheric wind variations (Song et al., 2007). Daily mean meridional winds (Fig. 4) exhibit oscillatory structure, indicative of planetary waves, in winter. We will present detailed analyses of the variation of zonal wind and the oscillatory structure of meridional wind in the following sub-sections.
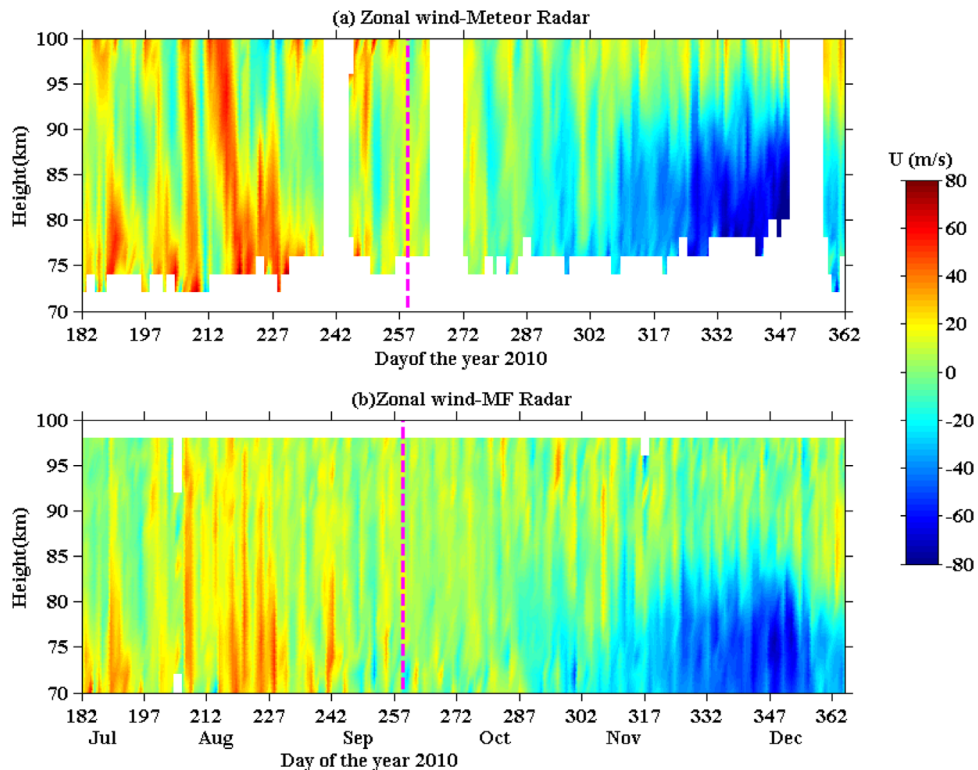

Fig. 3. Daily mean zonal winds obtained for the second half of the year (July–December) 2010 from (a) KSS meteor radar, and (b) Rothera MF radar.
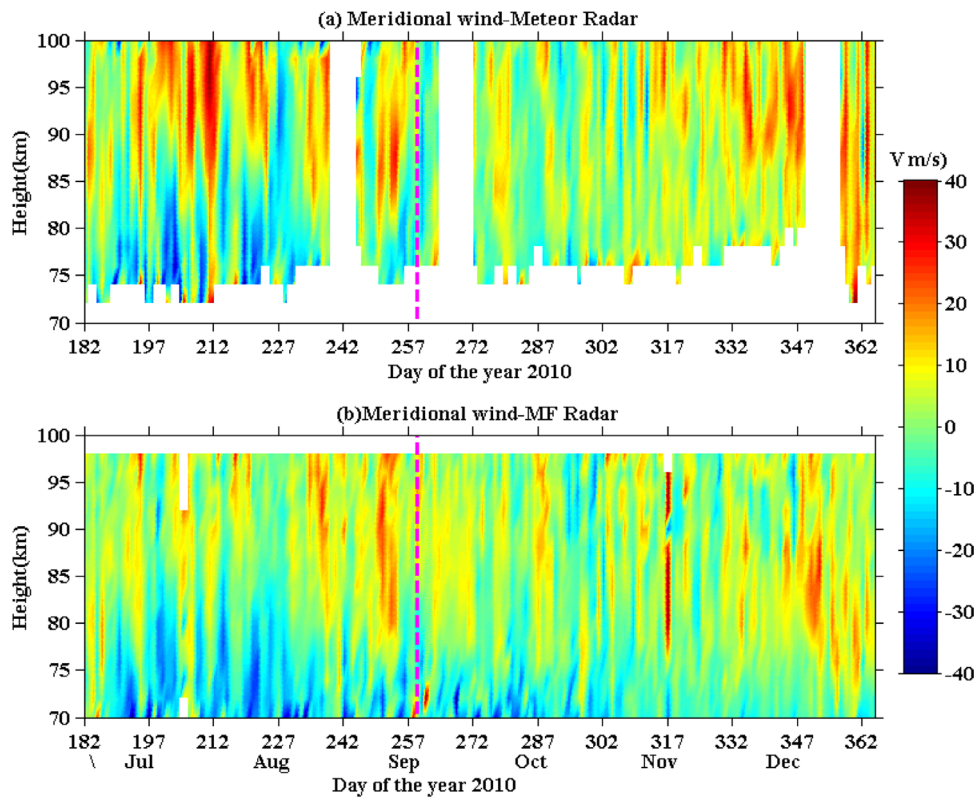
Fig. 4. Same as Fig. 3, but for meridional winds.

3.3. Stratosphere–mesosphere coupling

Fig. 5 shows the zonal mean zonal wind in the stratosphere and zonal winds in the mesosphere during the second half of 2010. The zonal winds in the stratosphere are obtained from ERA-Interim data and zonal winds in the mesosphere are observed from both the KSS MR and Rothera MF Radar. The variability of daily mean zonal winds of KSS MR and Rothera MF radar at 82 km are presented with black and blue lines, respectively. Zonal winds at 82 km of SD-WACCM also shown with green dotted line for comparison. There is good qualitative agreement between the model and the observed zonal wind variations A careful examination of Fig. 5 reveals that during the September minor SSW the wind reversal at KSS started on the day 251 (a week before the associated warming) and reached maximum magnitude (~ -10 m/s) on the day 253; and at Rothera station, the wind reversal started on the day 248 and reached its maximum values

(~ -8 m/s) on the day 252. Here we are using the term "wind reversal" for the occurrence of westward wind at 82 km. This one day difference in achieving maximum wind reversal can be explained with westward PW activity in the stratosphere. The mesosphere is responding to the PW activity which is controlling the stratospheric winds, which in turn are modulating the GW filtering and hence the mesospheric winds. The one day difference is most likely due to one station being more westward than the other. In effect the peak of the wave activity–zonal mean flow interaction in the stratosphere reaches the more westward station after one day. So the difference is due to longitudinal separation of the stations. The difference in wind magnitude can be attributed partly to the difference in wind measuring techniques. Usually MF radars tend to underestimate the winds than meteor radars (Rao et al., 2014). In the case of SD-WACCM the wind weakening at 82 km started along with radar observations of wind reversal, and became negative just a few days before the associated warming in
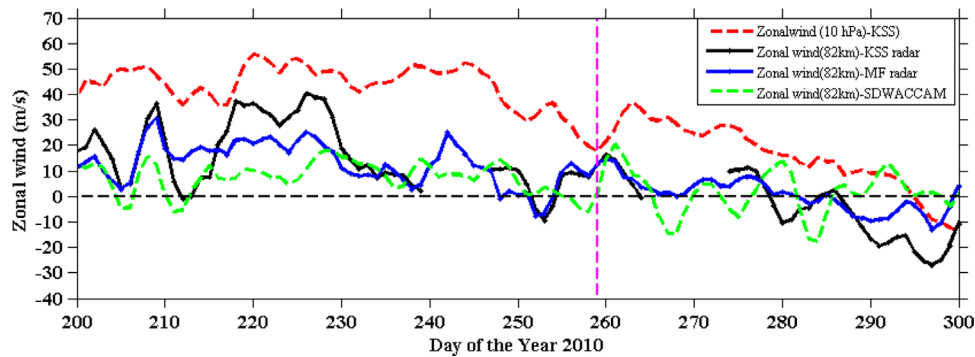

Fig. 5. Zonal mean zonal wind (dashed red line) at 32 km (10 hPa) obtained from ERA-Interim data set and zonal winds observed at 82 km (0.008 hPa) (black line) using KSS MR and Rothera MF radar (blue line). Zonal winds at 82 km of SD-WACCM are also shown with a green dotted line. The dashed horizontal line indicates the zero wind level and the vertical line indicates the day of peak warming. (For interpretation of the references to color in this figure legend, the reader is referred to the web version of this article.)

the stratosphere. After the SSW, an increase in eastward wind is observed for about 4–5 days before the seasonal transition. The zonal wind reversal observed with MF radar is quite consistent and clearer when compared to KSS MR observations (Fig. 5). We can also note the stratosphere–mesosphere coupling in the SD-WACCM simulation for the September event and reversal of zonal winds at ~82 km one week before the onset of the SSW (Fig. 2a), along with the weakening of the stratospheric jets due to increased stratospheric planetary wave activity. Although we noticed an episodic warming in early August, the mesospheric wind reversal was not recorded in either of radars. Similarly in October, the winds seem to be weakening down to negative values before the event, which can be regarded as seasonal change, not as wind reversal due to SSW. Hence the September warming is the clearest SSW event to show the dynamical impact on the mesosphere in 2010. This has been verified with a wavelet analysis of the meridional winds in the following sub-sections.

It is quite interesting that the wind reversal in the mesosphere for the 2010 minor SSW is similar in both magnitude and period to the major SSW event that occurred in 2002. During the 2002 SSW, the zonal wind was ~ − 10 m/s during the peak day (Dowdy et al., 2004; Mbatha et al., 2010), which is about the same magnitude of wind reversal during the September minor SSW event in our study. The wind reversal occurred a week before the 2002 event, as it did in the present case during the 2010 minor SSW.

3.4. Mean wind comparison with other years

In order to elucidate the mean wind difference between normal years and the SSW year we analyze the daily mean zonal winds at 82 km from both the KSS MR and Rothera radar during the second half of the year, as presented in Fig. 6. The zonal winds in 2010 are compared with mean winds along with standard deviations that were computed from the 7 year (2007–2014) dataset of the KSS MR and 10 year (2003–2013) dataset of the MF radar. The data were smoothed with 5-day running means in order to capture the clear variation between the 2010 and other years. The thick black line shows the average values of all years, excluding 2010. At both stations, the zonal winds at 82 km in 2010 are considerably different from the mean values observed in other years. Overall we notice more eastward winds in winter (August) and westward winds in summer (December) in 2010 than in other years. The 2010 zonal wind occasionally drifted off the standard deviation of the mean wind during August, October and December months, and also during the noted SSW. For instance, during the days 215–230, the zonal winds in 2010 were 10 m/s stronger than the other years mean wind; the 2010 zonal winds were reaching more than 40 m/s at KSS and 30 m/s at Rothera, whereas 2007–2014 and 2003–2013 mean winds stayed below 30 m/s, respectively. The wind reversal at 82 km a week before the associated SSW is clearly apparent in both the radar observations during September. The winter to summer zonal wind transition usually proceeds in early November, and the westward winds are in the range 20–30 m/s on average. However, during 2010 entirely different behavior occurred as zonal wind starts weakening during early October and becomes more westward at approximately day 290, and back to slightly eastward for about four days and then takes usual transition. Large wind fluctuations in July month (day 182–210) appear to be due to existence of strong 5–12 day waves in the background atmosphere at both stations and the wave features are discussed in next section. The daily averaged meridional winds (Figure not shown) in 2010 are close to the other year mean winds throughout the year, except just before the episodic warming events.
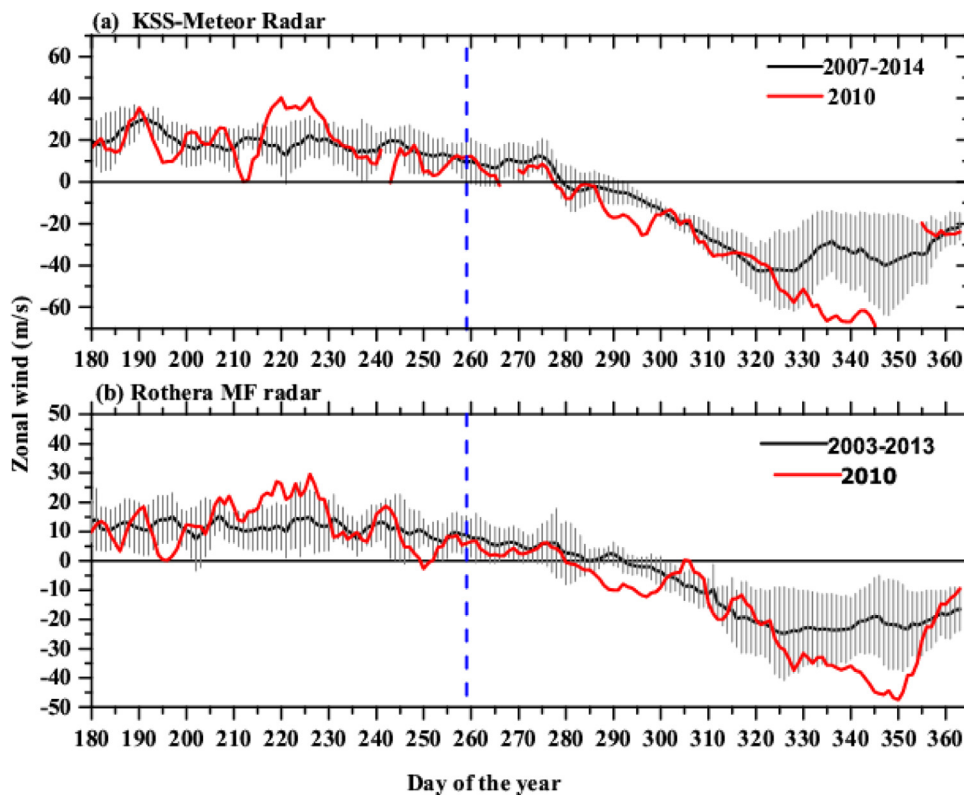

Fig. 6. (a) Five day running means of 7 year (2007–2014 except 2010) averaged zonal wind at 82 km (black line) and corresponding winds for the year 2010 (red line) from KSS radar. (b) Five day running means of 10 year (2003–2013 except 2010) averaged zonal wind at 82 km (black line) and corresponding winds for the year 2010 (red line) from MF radar. The standard deviation is shown in gray bars. The horizontal line indicates the zero wind level and the dashed vertical line indicates the day of peak warming. (For interpretation of the references to color in this figure legend, the reader is referred to the web version of this article.)
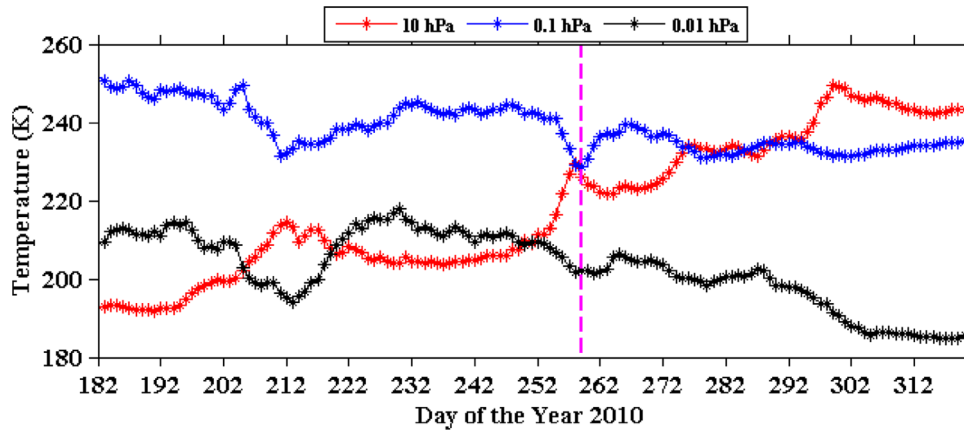
Fig. 7. Time series of the zonal mean temperature observed at 10 hPa, 0.1 hPa and 0.01 hPa by MLS at ∼80°S in 2010. A dashed vertical line indicates the day of peak warming.

3.5. Stratospheric warming–mesosphere cooling

Fig. 7 shows the time series of daily averaged zonal mean temperatures obtained from the MLS measurements at ∼80°S. The temperatures are presented for three pressure levels at 10 hPa, 0.1 hPa and 0.01 hPa to cover the stratosphere and the mesosphere during the 2010 period. Mesospheric cooling (MC) (at 0.1 hPa) is evident during the September event (at 10 hPa) and moderate cooling persists even up to 0.01 hPa. The MC can also be seen in early August in association with the episodic warming in stratosphere. The September SSW event clearly shows 18–20 K warming in stratosphere (10 hPa) for about a week. The magnitude of warming in stratosphere and associated cooling in mesosphere is rather similar to the 2002 major SSW event (Azeem et al., 2005; Ren et al., 2008; Hernandez, 2003). The firm anti-correlation between 0.1 hPa and 10 hPa temperatures during the minor SSW is consistent with earlier reports (Liu and Roble, 2002; Siskind et al., 2005). MC is also noticed in the SD-WACCM simulation at all the

episodic warming events (Fig. 2b), and it may be partly due to the breaking of more eastward traveling GWs reducing the down welling at mesospheric altitudes.

Liu and Roble (2002) suggested that the net strong westward forcing from PWs in the stratosphere will act on reversal of mesospheric jet and increase eastward forcing of GWs in mesosphere. The reversal of mesospheric jet results in change of mean meridional circulation from poleward/downward to equatorward/upward, leading to strong adiabatic cooling in the mesosphere at high latitudes. In the present case MC is noticed up to ∼78 to 80 km.

3.6. Planetary waves (PWs) during 2010 SSW

Clear link between PW activity and SSW has been suggested in previous studies (Matsuno, 1971; Andrews et al., 1987; Dowdy et al., 2004). In order to find PW activity in the mesospheric region before and after the 2010 SSW, we performed wavelet analysis for
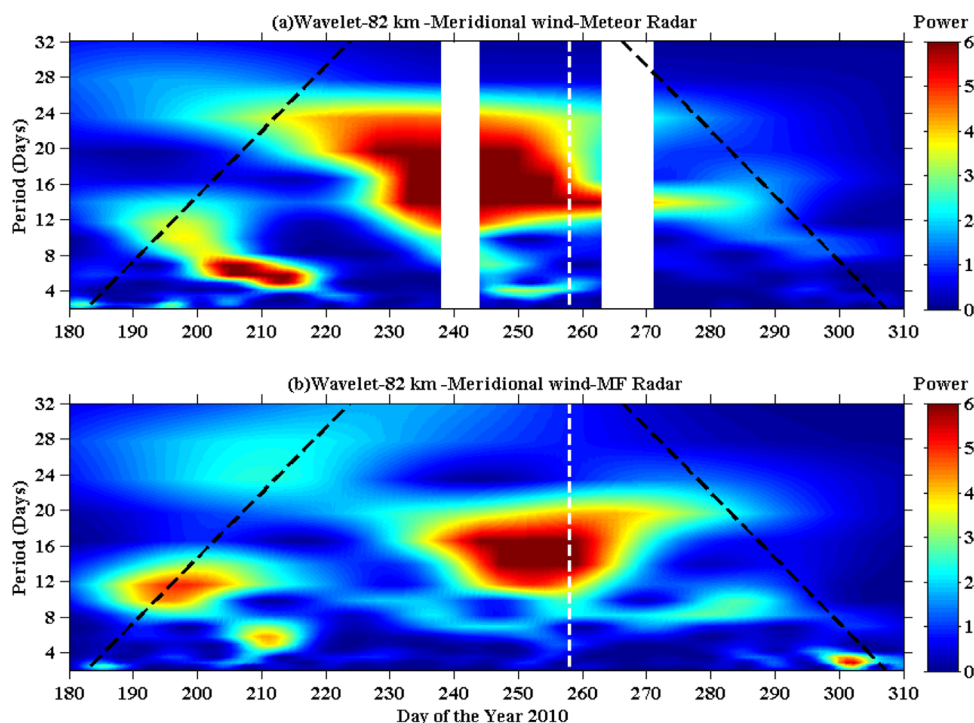

Fig. 8. Wavelet spectrum of meridional winds at 82 km observed in 2010, using (a) KSS radar (top), (b) MF radar (bottom). Dashed black line shows 95% confidence level and a vertical dashed white line shows the minor SSW event day. White patches in (a) indicates data gap.
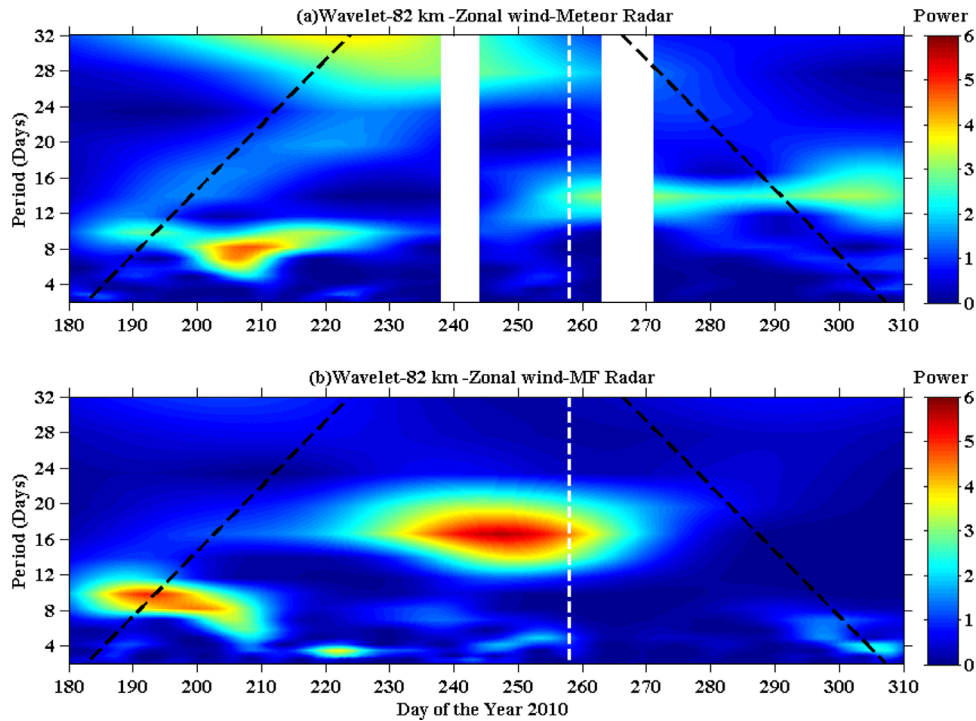
Fig. 9. Same as Fig. 8, but for zonal winds.

both the meridional and zonal winds at 82 km. The wavelet analysis was applied to the daily averaged winds from the day 180–310 to cover the entire winter period using both datasets of KSS MR and Rothera MF Radar. The wavelets of meridional winds are shown in Fig. 8a and b for data from KSS MR and Rothera MF Radar, respectively. The white patches in Fig. 8a indicate the data gaps. The figures indicate that the 14–16 day PWs reach to maximum amplitude a week before the onset of the September SSW, and these waves may be related to PWs in the stratosphere that cause the minor SSW. However, the 14–16 day waves were not present during August and October warmings in both stations. Note that Ratnam et al. (2004) reported enhanced gravity wave activity a few days before the SH major SSW that occurred in 2002, similar to that observed in the PW activity in the present case. During mid-July rather short period waves, 8–12 day and 5–8 day waves, seem to present over both stations in mid-July and early August, respectively, which may or may not be related to the August event. The wavelets of zonal winds are shown in Fig. 9a and b for data from KSS MR and Rothera MF Radar, respectively. In the zonal wind case 14–16 day waves are more apparent in MF radar data than the meteor radar data for the September event. We also verified the presence of waves in stratosphere during the 2010 disturbed winter using ERA-Interim data over the SH and are

shown in Fig. 10. The strong 14–16 day waves were dominant at 60°S (Fig. 10a), and 3–8 day (Fig. 10b) waves were growing and propagating poleward after the warmings in August and September. Hence the strong 14–16 day PWs observed during September event may be related to stratospheric PWs shown in Fig. 10.

After the September SSW event, the dominant wave weakens rapidly, and leaves behind secondary PWs with periods of 6–8 days that appears clearly in Fig. 8b. The occurrence of secondary PWs in the mesosphere, after the 2012 minor SSW event, was reported in the NH by Chandran et al. (2013). They found these short period planetary waves to be associated with sources of baroclinic instabilities in the upper stratosphere caused by vertical wind shears. Minor SSWs in the SH also produce the same phenomena observed in NH winters which affect mesospheric dynamics significantly.

4. Summary

The present communication describes the stratosphere–mesosphere coupling during the minor 2010 SSW in the SH using the simultaneous observations from KSS MR, Rothera MF radar and MLS temperature measurements. While studies on SSWs (both
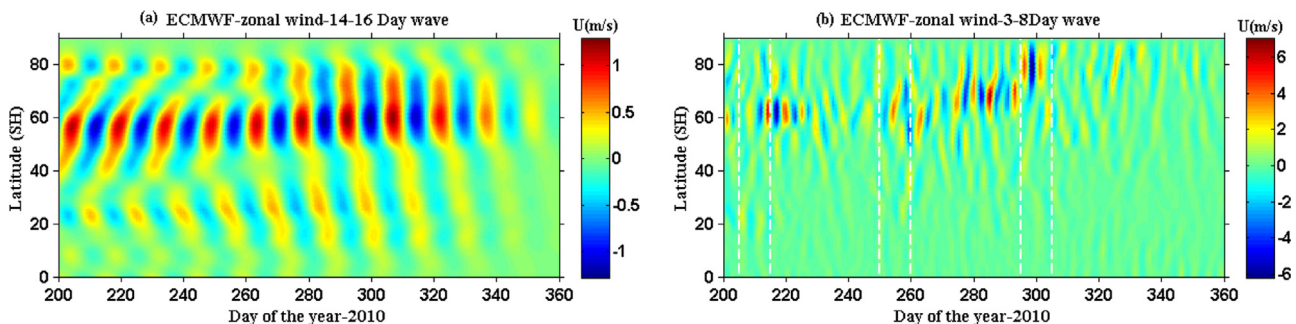

Fig. 10. (a) Propagation of 14–16 day waves observed in zonal winds at different latitudes in the SH using ECMWF data at 10 hPa. (b) Same as (a), but for 3–8 day wave propagation.

major and minor) and their effects on mesospheric dynamics are well established in the NH, relatively limited studies have been done in the SH due to both rare occurrence of SSW and few observational opportunities in the Antarctic region. Here, we present the observational features in the mesosphere over the Antarctic Peninsula during the minor warming event that occurred in September 2010. The main findings in the present study are summarized as follows;

1. A minor SSW was noticed on 16 September 2010 (day 259) along with small episodic warmings in August and October These observations are found to be consistent with previous studies on a SH minor warming using model forecasts (Coy et al., 2005; Siskind et al., 2010).
2. The comparison of daily mean zonal winds at 82 from both KSS MR and MF radar shows that wind reversal in mesosphere starts before (~eight days) the onset of the September SSW in conjunction with the stratospheric warming and wind reversal. The magnitude of wind reversal during the 2010 minor SSW is similar to that of the 2002 SH major SSW event. SD-WACCM simulations clearly captured the weakening of zonal wind at ~40 km and the wind reversal at ~82 km before the SSW for the September minor SSW. The mean zonal wind structure in the mesosphere measured from both stations in 2010 is significantly different from that of other years.
3. The MLS dataset clearly showed the mesospheric cooling (MC) at 0.1 hPa, which is strongly associated with the minor SSW. This anti-correlation is even extended to upper mesosphere (0.01 hPa). We also noticed MC for the corresponding stratosphere warmings in the SD-WACCM simulation. Earlier reports (Azeem et al., 2005; Ren et al., 2008) have well documented MC during the major 2002 SSW, which can be attributed to net upwelling and associated adiabatic cooling due to changes in the gravity wave drag.
4. Strong PWs in association with the minor SSW is found. Strong 14–16 day PWs were present prior to the September SSW but disappeared suddenly after the SSW, leaving behind secondary planetary waves (6–8 day) in the mesosphere. The behavior of PWs in association with SSW events is consistent with the current idea that SSWs are caused by interaction of PW with mean flow.

Thus, the main conclusion that can be drawn from the present study is that, the 2010 minor SSW in the SH produced changes in polar mesospheric winds and temperature comparable to the 2002 major SSW.

Acknowledgments

References

Andrews, D.G., Holton, J.R., Leovy, C.B., 1987. Middle Atmosphere Dynamics. Academic, San Diego, California, pp. 129–130.

Azeem, S.M.I., Talaat, E.R., Sivjee, G.G., Liu, H.-L., Roble, R.G., 2005. Observational study of the 4-day wave in the mesosphere preceding the sudden stratospheric warming events during 1995 and 2002. Geophys. Res. Lett. 32, L15804. http://dx.doi.org/10.1029/ 2005GL023393.

Baldwin, M.P., Hirooka, T., O'Neill, A., Yoden, S., Charlton, A.J., Hio, Y., Lahoz, W.A., Mori, A., 2003. Major stratospheric warming in the southern hemisphere in 2002: dynamical aspects of the ozone hole split, SPARC newsletter. 20. SPARC Office, Toronto, ON, Canada, pp. 24–26.

Chandran, A., Collins, R.L., Harvey, V.L., 2014. Review on Stratosphere–mesosphere coupling during stratospheric sudden warming events. Adv. Space Res. 53 (2014), 1265–1289.

Chandran, A., Garcia, R.R., Collins, R.L., Chang, L.C., 2013. Secondary planetary waves in the middle and upper atmosphere following the stratospheric sudden warming event of January 2012. Geophys. Res. Lett. 40, 1861–1867. http://dx.doi.org/10.1002/grl.50373.

Charlton, A.J., Polvani, L.M., 2007. A new look at stratospheric sudden warmings. Part I. Climatology and modeling bench marks. J. Climate 20, 449–469.

Cho, Y.-M., Shepherd, G.G., Won, Y.-I., Sargoytchev, S., Brown, S., Solheim, B., 2004. MLT cooling during stratospheric warming events. Geophys. Res. Lett. 31, L10104. http://dx.doi.org/10.1029/2004GL019552.

Coy, L., Siskind, D.E., Eckermann, S.D., McCormack, J.P., Allen, D.R., Hogan, T.F., 2005. Modeling the august 2002 minor warming event. Geophys. Res. Lett. 32, L07808. http://dx.doi.org/10.1029/2005GL022400.

De la Torre, L., Garcia, R.R., Barriopedro, D., Chandran, A., 2012. Climatology and characteristics of stratospheric sudden warmings in the whole atmosphere community climate model. J. Geophys. Res. 117. http://dx.doi.org/10.1029/2011JD016840.

Dee, et al., 2011. The ERA-interim reanalysis: configuration and performance of the data assimilation system. Q. J. R. Meteorol. Soc. 137, 553–597. http://dx.doi.org/10.1002/qj.828.

Dowdy, A.J., Vincent, R.A., Murphy, D.J., Tsutsumi, M., Riggin, D.M., Jarvis, M.J., 2004. The large-scale dynamics of the mesosphere–lower thermosphere during the southern hemisphere stratospheric warming of 2002. Geophys. Res. Lett. 31, L14102. http://dx.doi.org/10.1029/ 2004GL020282.

Fairlie, T.D.A., Fisher, M., O'Neill, A., 1990. The development of narrow baroclinic zones and other small-scale structure in the stratosphere during simulated major warmings. Q. J. R. Meteorol. Soc. 116, 287–315. http://dx.doi.org/10.1002/qj.49711649204.

Garcia, R.R., Marsh, D.R., Kinnison, D.E., Boville, B.A., Sassi, F., 2007. Simulation of secular trends in the middle atmosphere, 1950–2003. J. Geophys. Res. 112, D09301. http://dx.doi.org/10.1029/2006JD007485.

Greer, K., Thayer, J.P., Harvey, V.L., 2013. A climatology of polar winter stratopause warmings and associated planetary wave breaking. J. Geophys. Res. Atmos. 118, 4168–4180. http://dx.doi.org/10.1002/jgrd.50289.

Hernandez, G., 2003. Climatology of the upper mesosphere temperature above South Pole (90°S): mesospheric cooling during 2002. Geophys. Res. Lett. 30 (10), 1535. http://dx.doi.org/10.1029/2003GL016887.

Hibbins, R.E., Espy, P.J., Jarvis, M.J., Riggin, D.M., Fritts, D.C., 2007. A climatology of tides and gravity wave variance in the MLT above Rothera, antarctica obtained by MF radar. J. Atmos. Solar-Terr. Phys. 69, 578–588.

Holdsworth, D.A., Reid, I.M., Cervera, M.A., 2004. Buckland Park all- sky interferometric meteor radar. Radio Sci. 39 (5). http://dx.doi.org/10.1029/2003RS003014.

Hoppel, K., Bevilacqua, R., Allen, D.D., Nedoluha, G., Randall, C., 2003. POAM III observations of the anomalous 2002 Antarctic ozone hole. Geophys. Res. Lett. 30, 1394. http://dx.doi.org/10.1029/ 2003GL016899.

Hu, Y., Fu, Q., 2009. Stratospheric warming in Southern Hemisphere high latitudes since 1979. Atmos. Chem. Phys. 9, 4329–4340. http://dx.doi.org/10.5194/acp−9−4329−2009.

Jarvis, M.J., Jones, G.O.L., Jenkins, B., 1999. New initiatives in observing the Antarctic mesosphere. Adv. Space Res. 24 (5), 611–619.

Kawahara, T.D., Gardner, C.S., Nomura, A., 2004. Observed temperature structure of the atmosphere above Syowa Station, Antarctica (69°S, 39°E). J. Geophys. Res. 109, D12103. http://dx.doi.org/10.1029/2003JD003918.

Kim, J.-H., Kim, Y.H., Lee, C.S., Jee, G., 2010. Seasonal variation of meteor decay times observed at King Sejong Station (62.22°S, 58.78°W), Antarctica. J. Atmos. Solar-Terr. Phys. 72 (11–12), 883–889.

Kishore, P., Velicogna, I., Ratnam, M.V., Jiang, J.H., Madhavi, G.N., 2012. Planetary waves in the upper stratosphere and lower mesosphere during 2009 Arctic major stratospheric warming. Ann. Geophys. 30, 1529–1538.

Labitzke, K., 1972. Temperature changes in the mesosphere and stratosphere connected with circulation changes in winter. J. Atmos. Sci. 29, 756–766.

Labitzke, K., Naujokat, B., 2000. The lower arctic stratosphere in winter since 1952. SPARC Newsl. 15, 11–14.

Lee, C., Kim, Y.H., Kim, J.-H., Jee, G., Won, Y.-I., Wu, D.L., 2013. Seasonal variation of wave activities near the mesopause region observed at King Sejong station (62.22°S, 58.78°W). Antarcti. J. Atmos. Sol-Terr. Phys. 105–106, 30–38.

Liu, H.-L., Roble, R.G., 2002. A study of a self-generated stratospheric sudden warming and its mesospheric–lower thermospheric impacts using the coupled TIME-GCM/CCM3. J. Geophys. Res. 107 (D23), 4695. http://dx.doi.org/10.1029/2001JD001533.

Manney, G.L., Schwartz, M.J., Krüger, K., Santee, M.L., Pawson, S., Lee, J.N., Daffer, W. H., Fuller, R.A., Livesey, N.J., 2009. Aura microwave limb sounder observations of dynamics and transport during the record-breaking 2009. Arctic stratospheric major warming. Geophys. Res. Lett. 36, L12815. http://dx.doi.org/10.1029/2009GL038586.

Manson, A.H., Meek, C.E., Hall, C.M., Nozawa, S., Mitchell, N.J., Pancheva, D., Singer, W., Hoffmann, P., 2004. Mesopause dynamics from the scandinavian triangle of radars within the PSMOS-DATAR project. Ann. Geophys. 22, 367–386.

Marsh, Daniel R., Mills, M., Kinnison, D., Lamarque, J.-F., Calvo, N., Polvani, L., 2013. Climate change from 1850 to 2005 simulated in CESM1 (WACCM). J. Climate 26, 7372–7391. http://dx.doi.org/10.1175/JCLI-D-12-00558.1.

Matsuno, T.A., 1971. Dynamical model of the stratospheric sudden warming. J. Atmos. Sci. 28, 1479–1494.

Mbatha, N., Sivakumar, V., Malinga, S.B., Bencherif, H., Pillay, S.R., 2010. Study on the impact of sudden stratosphere warming in the upper mesosphere–lower thermosphere regions using satellite and HF radar measurements. Atmos. Chem. Phys. 10, 3397–3404. http://dx.doi.org/10.5194/acp-10-3397-2010.

Mthembu, S.H., Sivakumr, V., Mitchell, N.J., Malinga, S.B., 2013. Studies on planetary waves and tide interaction in the mesosphere/lower thermosphere region using meteor RADAR data from Rothera (68°S, 68°W), antarctica. J. Atmos. Solar Terr. Phys. 102, 59–73.

Pan, W., Gardner, C.S., 2003. Seasonal variations of the atmospheric temperature structure at south pole. J. Geophys. Res. 108 (D18), 4564. http://dx.doi.org/10.1029/2002JD003217.

Portnyagin, Yu.I., Solovjova, T.V., Makarov, N.A., Merzlyakov, E.G., Manson, A.H., Meek, C.E., Hocking, W., Mitchell, N.J., Pancheva, D., Hoffmann, P., Singer, W., Murayama, Y., Igarashi, K., Forbes, J.M., Palo, S., Hall, C., Nozawa, S., 2004. Monthly mean climatology of the prevailing winds and tides in the arctic mesosphere/lower thermosphere. Ann. Geophys. 22, 3395–3410.

Rao, S.V.B., Eswaraiah, S., Venkat Ratnam, M., Kosalendra, E., Kishore Kumar, K., Sathish Kumar, S., Patil, P.T., Gurubaran, S., 2014. Advanced meteor radar installed at Tirupati: system details and comparison with different radars. J. Geophys. Res. Atmos. 119. http://dx.doi.org/10.1002/2014JD021781.

Ren, S., Polavarapu, S.M., Shepherd, T.G., 2008. Vertical propagation of information in a middle atmosphere data assimilation system by gravity-wave drag feedbacks. Geophys. Res. Lett. 35, L06804. http://dx.doi.org/10.1029/2007GL032699.

Richter, J.H., Sassi, F., Garcia, R.R., 2010. Toward a physically based gravity wave source parameterization in a general circulation model. J. Atmos. Sci. 67, 136–156. http://dx.doi.org/10.1175/2009JAS3112.1.

Rienecker, M. M. et al., (2008). The GEOS-5 data assimilation system – documentation of versions 5.0.1, 5.1.0, and 5.2.0. NASA/TM-2008-104606. Vol. 27, Technical Report Series on Global Modeling and Data Assimilation. p. 118.

Scherhag, R., 1952. Die explosionsartigen stratospärenerwärmungen des spätwinters 1951 – 1952. Ber. Dtsch. Wetterd. 6, 51–63.

Schwartz, M.J., et al., 2008. Validation of the aura microwave limb sounder temperature and geopotential height measurements. J. Geophys. Res. 113, D15S11. http://dx.doi.org/10.1029/2007JD008783.

Shepherd, T., Plumb, R.A., Wofsy, S.C., 2005. Preface to JAS special issue on the antarctic stratospheric sudden warming and split ozone hole of 2002. J. Atmos. Sci. 62, 565–566. http://dx.doi.org/10.1175/JAS-9999.1.

Siskind, D.E., Coy, L., Espy, P., 2005. Observations of stratospheric warmings and mesospheric coolings by the TIMED SABER instrument. Geophys. Res. Lett. 32, L09804. http://dx.doi.org/10.1029/2005GL022399.

Siskind, D.E., Eckermann, S.D., McCormack, J.P., Coy, L., Hoppel, K.W., Baker, N.L., 2010. Case studies of the mesospheric response to recent minor, major, and extended stratospheric warmings. J. Geophys. Res. 115, D00N03. http://dx.doi.org/10.1029/2010JD014114.

Song, In-Sun, Chun, Hye-Yeong, Garcia, Rolando R., Boville, Byron A., 2007. Momentum flux spectrum of convectively forced internal gravity waves and its application to gravity wave drag parameterization. Part II: impacts in a GCM (WACCM). J. Atmos. Sci. 64, 2286–2308. http://dx.doi.org/10.1175/JAS3954.1.

Thayer, J.P., Livingston, J.M., 2008. Observations of wintertime arctic mesosphere cooling associated with stratosphere baroclinic zones. Geophys. Res. Lett. 35, L18803. http://dx.doi.org/10.1029/2008GL034955.

Ratnam, M. Venkat, Aoyama, Y., Tsuda, T., Jacobi, Ch, 2004. Enhancement of gravity wave activity observed during a major southern hemisphere stratospheric warming by CHAMP/GPS measurements. Geophys. Res. Lett. 31, L16101. http://dx.doi.org/10.1029/2004GL019789.

de Laat, A.T.J., van Weele, M., 2011. The 2010 antarctic ozone hole: observed reduction in ozone destruction by minor sudden stratospheric warmings. Sci. Rep. 1, 38. http://dx.doi.org/10.1038/srep00038 (2011).

de Wit, R.J., Hibbins, R.E., Espy, P.J., Hennum, E.A., 2015. Coupling in the middle atmosphere related to the 2013 major sudden stratospheric warming. Ann. Geophys. 33, 309–319. http://dx.doi.org/10.5194/angeo-33-309-2015.

von Zahn, U., Fiedler, J., Naujokat, B., Langematz, U., Krüger, K., 1998. A note on record-high temperatures at the northern polar stratopause in winter 1997/98. Geophys. Res. Lett. 25, 4169–4172. http://dx.doi.org/10.1029/1998GL900091.